An X-ray Reflectivity Study of the Water-Docosane Interface

Aleksey M. Tikhonov,[†] Dragoslav M. Mitrinovic,[†] Ming Li,[†] Zhengqing Huang,[‡] and Mark L. Schlossman*[,†,§]

Departments of Physics and Chemistry, University of Illinois at Chicago, 845 West Taylor St., Chicago, Illinois 60607, and National Synchrotron Light Source, Brookhaven National Laboratory, Upton, New York 11973

Received: April 10, 2000; In Final Form: May 25, 2000

Synchrotron X-ray reflectivity is used to study the electron density profile normal to the interface between bulk water and bulk *n*-docosane ($C_{22}H_{46}$). These measurements are interpreted in terms of an error function electron density profile to yield an interfacial width of 5.7 ± 0.2 Å. In contrast with an earlier measurement on the water−hexane interface, this interfacial width disagrees sharply with the prediction from capillary wave theory, $\sigma_{cap} = 3.5$ Å. This width can be accounted for by combining the capillary wave prediction with a contribution from intrinsic structure due to the bulk correlation length of docosane. We also discuss the absence of interfacial freezing at this interface, a phenomenon observed for *n*-alkanes of a similar chain length at the alkane−vapor and alkane−silicon oxide interfaces.

Introduction

An outstanding problem in the area of interfacial phenomena is the determination of structure at liquid−liquid interfaces. This structure is relevant, for example, to the understanding of electron and molecular transfer across biological membranes and the partitioning of solvents and metal ions across liquid−liquid interfaces. The water−alkane interface is an important model system for understanding interactions between hydrocarbon chains and water and is, therefore, of relevance to biological and technological interfacial phenomena. Optical reflection second-harmonic generation has been used to probe the molecular ordering of *n*-alkanes (carbon numbers 7−10) at the water−alkane interface.[1] Here, we present an X-ray reflectivity study of the interface between bulk liquid water and bulk liquid *n*-docosane ($C_{22}H_{46}$).

We previously reported a measurement of the interfacial width between water and hexane.[2] This width was shown to be in agreement with a prediction from capillary wave theory. Here, we show that a significant deviation from the prediction of capillary wave theory occurs for the water interface with a longer chain alkane, *n*-docosane. The measured width can be explained by combining the capillary wave contribution to the interfacial width with a contribution from the bulk docosane correlation length.

Ordering at the interface of *n*-alkanes with solid silicon oxide and surface freezing at the vapor interface of liquid alkanes have also been reported recently.[3−5] At the vapor interface, systematic studies have shown that a single layer freezes at the alkane surface within approximately 2−3 °C above the bulk freezing temperature.[6] This freezing occurs for *n*-alkanes with chain lengths in the range from 16 to 50 carbons long. A related observation, also for chain lengths from 16 to 50 carbons, was reported for thin films of *n*-alkanes on the surface of SiO_2.[5]

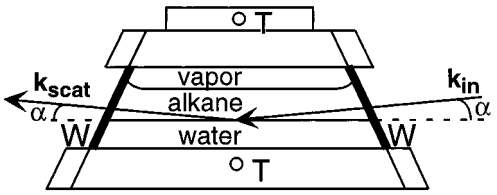

Figure 1. Cross-sectional view of sample cell: W, Mylar windows; T, thermistors to measure temperature. The kinematics of surface X-ray reflectivity is also indicated: $\boldsymbol{k}_{in}$ is the incoming X-ray wave vector, $\boldsymbol{k}_{scat}$ is the scattered wave vector, and α is the angle of incidence and reflection.

Here, we use interfacial tension and X-ray reflectivity measurements to demonstrate the absence of interfacial freezing at the water−docosane ($C_{22}H_{46}$) interface.

Experimental Methods

The measurements presented here are from liquid samples that are stirred and allowed to reach thermal equilibrium in a vapor-tight stainless steel sample cell, which is discussed in detail elsewhere.[2,7,8] High-purity water was produced from a Barnstead NanoPure system; *n*-docosane (99.2%, purum grade) was purchased from Fluka. Docosane was further purified by passing it several times through a heated (60−70 °C) column of basic alumina.[9] The interfacial tension was measured with a Wilhelmy plate in the same sample cell used for the X-ray measurements. At fixed temperature, the tension between docosane and water was constant to within ±0.1 dyn/cm as a function of time, where time is measured from the initial formation of the water−alkane interface. Without the purification step, there was significant adsorption of impurities to the water−docosane interface, as indicated by a change in the interfacial tension of approximately 15 dyn/cm over a period of a few hours.

The interfacial area was 76 mm × 100 mm (along the beam × transverse) with X-rays penetrating through the upper phase (see Figure 1). At the chosen X-ray wavelength ($\lambda = 0.825 \pm 0.002$ Å) the absorption lengths for docosane and water are 18

* Author to whom correspondence should be addressed. E-mail: schloss@uic.edu.
[†] Department of Physics.
[‡] Brookhaven National Laboratory.
[§] Department of Chemistry.

10.1021/jp001377u CCC: $19.00
Published on Web 00/00/0000 PAGE EST: 3.2

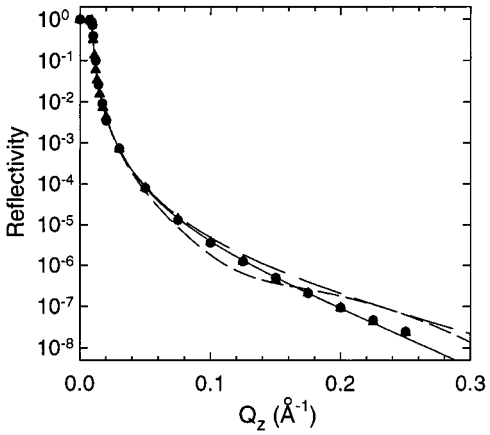

Figure 2. X-ray reflectivity of water−docosane interface. Filled circles and triangles are measurements at $T = 44.6$ °C (circles) and $T = 51.6$ °C (triangles). Solid line through the data points is a one-parameter fit to the 44.6 °C data (see eq 2 and text). Long-dashed line is the calculated reflectivity when the width is determined solely by capillary waves. Short-dashed line is the calculated reflectivity assuming a single layer of frozen docosane at the water−docosane interface.

and 5.6 mm, respectively. The sample cell is contained in a one-stage cylindrical aluminum thermostat and temperature controlled to ±0.03 °C. Two thermistors mounted immediately above and below the liquid chamber measure the sample temperature and allow us to determine when the sample cell has thermally equilibrated.

X-ray reflectivity was conducted at beamline X19C at the National Synchrotron Light Source (Brookhaven National Laboratory, Upton, NY) with a liquid surface spectrometer and measurement techniques described in detail elsewhere.[7,10] The kinematics of reflectivity is illustrated in Figure 1; note that α = 90° is normal to the surface. For specular reflection, the wave vector transfer, $\boldsymbol{Q} = \boldsymbol{k}_{scat} - \boldsymbol{k}_{in}$, is only in the z direction, normal to the interface; $Q_x = Q_y = 0$, where x and y are in the plane of the interface, and $Q_z = (4\pi/\lambda) \sin \alpha$.

To set the incident beam size and reduce the vertical divergence to 20 μrad, two slits placed approximately 60 cm apart were used immediately prior to the liquid sample. The slit gaps were typically 5−10 μm in the vertical direction at the smallest reflection angles (horizontal slit gaps were 10 mm, much larger than the horizontal beam size of ∼2 mm). A scintillator monitor immediately in front of the sample measured the incident X-ray flux. The sample was followed by a slit with a vertical gap of ∼2 mm to reduce the background scattering, and the scintillator detector was preceded immediately by a slit with a vertical gap of either 0.4 or 0.6 mm, which set the detector resolution.

X-ray Data and Analysis

Figure 2 illustrates the X-ray reflectivity measurements for the water−docosane interface at two different temperatures, 44.6 and 51.6 °C, both above the bulk melting temperature of docosane, $T_{melt} = 44.1 \pm 0.2$ °C, that we measured for our sample.[11] The X-ray measurements at these two temperatures agree within error bars. Below a critical wave vector transfer for total reflection, Q_c, the reflectivity is nearly one; above Q_c, the reflectivity drops off rapidly with increasing Q_z. Reflectivity measurements of this form can be fit using one parameter, σ, that represents the width of an error function interfacial profile. This profile describes the variation in electron density as a function of the normal coordinate z through the water−alkane interface, given by

$$\langle\rho(z)\rangle = \frac{1}{2}(\rho_w + \rho_d) + \frac{1}{2}(\rho_w - \rho_d)\,\mathrm{erf}[z/\sigma\sqrt{2}] \text{ with } \mathrm{erf}(z) = \frac{2}{\sqrt{\pi}}\int_0^z e^{-t^2}\,dt \quad (1)$$

where $\langle\rho(z)\rangle$ is the interfacial electron density averaged over the plane of the interface and ρ_w and ρ_d represent the electron densities (normalized to the value for water) of bulk water and docosane, respectively. For this interfacial profile, the reflectivity can be written, for $Q_z > Q_c$,[12,13] as

$$R(Q_z) \cong \left|\frac{Q_z - Q_z^T}{Q_z + Q_z^T}\right|^2 \exp(-Q_z Q_z^T \sigma^2) \quad (2)$$

where $Q_z^T \cong \sqrt{Q_z^2 - Q_c^2}$ is the z component of wave vector transfer with respect to the lower phase. The critical wave vector transfer, Q_c, is calculated from the bulk densities as $Q_c = 4[\pi r_e(\rho_w - \rho_{al})]^{1/2} = 0.00963$ Å^{-1} (where $r_e = e^2/mc^2$), in agreement with our measurements. A fit of the data to eq 2 using a single fitting parameter, σ, is illustrated by the solid line in Figure 2 and yields the interfacial width $\sigma = 5.7 \pm 0.2$ Å for both temperatures.

Discussion

In the spirit of a hybrid model of the interface that describes an intrinsic structural profile roughened by capillary waves, the interfacial width, σ, can be represented as a combination of an intrinsic profile width, σ_o, and a resolution-dependent, capillary wave contribution[14−19]

$$\sigma^2 = \sigma_o^2 + \frac{k_B T}{4\pi^2\gamma}\int\int \frac{d^2\mathbf{q}}{q^2 + \xi_{||}^{-2}} \equiv \sigma_o^2 + \sigma_{cap}^2 \quad (3)$$

where $k_B T$ is Boltzmann's constant times the temperature; γ is the measured interfacial tension; the correlation length, $\xi_{||}$, is given by $\xi_{||}^2 = \gamma/\Delta\rho_m g$ and determines the exponential decay of the interfacial correlations given by the height−height correlation function of interfacial motion;[20] $\Delta\rho_m$ is the *mass* density difference of the two phases, and g is the constant of gravitational acceleration. Integration is over in-plane capillary wave vectors $\boldsymbol{q}$ corresponding to the range of capillary waves that the measurement probes. After some simplifications, the capillary contribution evaluates to $\sigma_{cap}^2 = k_B T/(2\pi\gamma) \log(q_{max}/q_{min})$, where q_{max} is determined by the cutoff for the smallest wavelength capillary waves that the interface can support and $q_{min} = (2\pi/\lambda)\Delta\beta \sin\alpha$ is determined by the incident angle α and the angular acceptance of the detector $\Delta\beta$.[21]

The capillary wave contribution to the interfacial width, σ_{cap}, calculated from the interfacial tension (measured with a Wilhelmy plate) and eq 3 is $\sigma_{cap} \cong 3.5$ Å, significantly different from our measured value for the interfacial width, $\sigma = 5.7 \pm 0.2$ Å.[22] A calculated prediction for the reflectivity based on only the capillary wave contribution to the interfacial width is shown in Figure 2. At the highest value of Q_z, the measured reflectivity is a factor of 3 lower than the prediction from capillary wave theory. This deviation is easily measured.

For long-chain polymers, it has been shown that adsorption of a polymer melt against a hard wall should be governed by a bulk correlation length, $\xi_b \sim \rho_b^{-1/2}$, which we write as $\xi_b = C_b(l\rho_b)^{-1/2}$, where ρ_b is the bulk monomer number density, C_b is an adjustable parameter of order 1, and l =1.54 Å is the carbon−carbon bond length.[23] Letting $C_b = 1$ yields $\xi_b = 4.4$ Å, which is very close to the chain−chain separation in

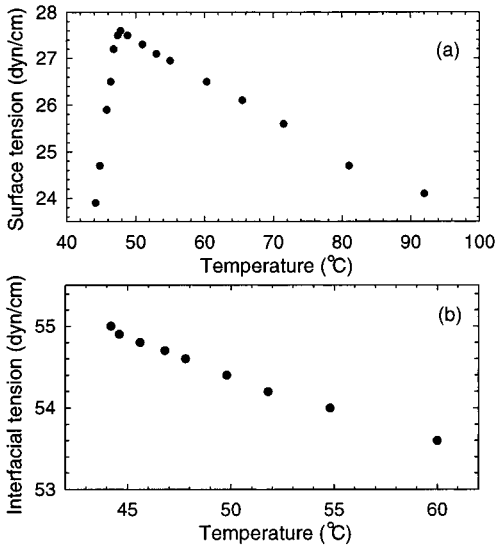

Figure 3. (a) Docosane−vapor surface tension. (b) Water−docosane interfacial tension.

hydrocarbon liquids of 4.6 Å.[24,25] If we regard this bulk correlation length as setting the length scale for the interfacial width due to intrinsic structure, σ_o, then the total interfacial width can be calculated by adding in quadrature the contributions to the width from intrinsic structure and capillary waves (see eq 3). The width, σ, calculated in this way is $\sigma = 5.6$ Å, in agreement with our measured value of 5.7 ± 0.2 Å.

To test for the possibility of an interfacial alkane freezing analogous to the alkane surface freezing previously reported, we measured reflectivity from the water−docosane interface at temperatures 0.5 and 7.5 °C above the bulk melting temperature ($T = 44.6$ and 51.6 °C, respectively). Measurements at the alkane−vapor interface have shown that the topmost layer of alkane freezes approximately 3 °C (3.13 °C for docosane) above the bulk melting temperature and only that single layer remains frozen as the temperature is lowered until the bulk freezes.[6] A possibly related freezing occurs for a single monolayer of alkane on solid SiO_2. There, the layer is frozen until the temperature is raised to approximately 3.5 °C above the bulk melting temperature.[5] In both of these cases, the frozen alkane monolayer contains ordered alkanes with their chains oriented normal to the surface. A recent model for surface freezing relies upon this orientation of the alkane chains. It was proposed that translational fluctuations along the molecular axis of the stretched alkanes provide sufficient entropy to stabilize the solid monolayer.[26]

If these surface freezing measurements are a guide, then by choosing to measure at temperatures 0.5 and 7.5 °C above the bulk melting temperature, we have bracketed the temperature range in which an interfacial freezing transition of the alkane might be expected. The frozen monolayer should have the docosane oriented normal to the interface. Figure 2 illustrates the calculated reflectivity that would be expected from this frozen monolayer (on the basis of the measured electron density for a frozen docosane monolayer at the vapor interface[6]). As can be seen from Figure 2, these data eliminate the possibility of a frozen layer of interfacial docosane oriented normal to the interface at these temperatures.

Figure 3 illustrates the interfacial (water−docosane) and surface (docosane−vapor) tensions as a function of temperature. The surface tension (Figure 3a) illustrates the characteristic break in slope that indicates the onset of surface freezing.[27] The constant slope in the interfacial tension vs temperature plot (Figure 3b, water−docosane) indicates that the excess interfacial entropy $S^i = -d\gamma/dT$ is constant and provides no evidence for an interfacial phase transition. This combination of X-ray reflectivity and interfacial tension measurements indicates an absence of interfacial freezing at a temperature above the bulk freezing temperature. These measurements reveal a significant difference between alkane ordering at the interface with vapor or with water.

We have shown that the bulk correlation length sets the length scale for the intrinsic structure that contributes to the interfacial width of the water−docosane interface. Measurements of the surface nonlinear susceptibility using optical second harmonic generation at the water−alkane interface for shorter *n*-alkanes (C7−C10) suggest that these interfaces may be highly ordered.[1] If similar ordering exists for this longer alkane (C22), then it is sensible to expect that this molecular order is related to the intrinsic structure that we have measured. As just discussed, our results exclude the possibility that this ordering is due to a perpendicular orientation of the molecules to the interface. Because of current limitations in the experimental range of Q_z, it is not possible to test whether some molecular ordering arises from molecules preferentially oriented parallel to the surface. Models of our data that include molecular layering parallel to the interface require more than one layer to fit our data, and such a complex interface is not justified by our current measurements. In addition, our interfacial tension measurements indicate the absence of an interfacial phase transition distinct from the bulk freezing transition in which alkane molecules order parallel to the interface.

We have also measured the interfacial width at the water−alkane interface for *n*-alkanes with lengths between those of hexane and docosane.[28] For shorter chain lengths, the interfacial width varies with carbon number, leading to a crossover between the interfacial width for the water−hexane interface, determined by capillary waves, and the larger interfacial width at the water−docosane interface that is due to both intrinsic structure and capillary waves.

Acknowledgment. We thank Sai Venkatesh Pingali for help in purifying the docosane. This work was supported by the donors of the Petroleum Research Fund administered by the ACS, the UIC Campus Research Board, and the NSF Division of Materials Research. Brookhaven National Laboratory is supported by the U.S. Department of Energy.

References and Notes

(1) Conboy, J. C.; Daschbach, J. L.; Richmond, G. L. *J. Phys. Chem.* **1994**, *98*, 9688.

(2) Mitrinovic, D. M.; Zhang, Z.; Williams, S. M.; Huang, Z.; Schlossman, M. L. *J. Phys. Chem.* **1999**, *103*, 1779.

(3) Wu, X. Z.; Sirota, E. B.; Sinha, S. K.; Ocko, B. M.; Deutsch, M. *Phys. Rev. Lett.* **1993**, *70*, 958.

(4) Ocko, B. M.; Wu, X. Z.; Sirota, E. B.; Sinha, S. K.; Deutsch, M. *Phys. Rev. Lett.* **1994**, *72*, 242.

(5) Merkl, C.; Pfohl, T.; Riegler, H. *Phys. Rev. Lett.* **1997**, *79*, 4625.

(6) Ocko, B. M.; Wu, X. Z.; Sirota, E. B.; Sinha, S. K.; Gang, O.; Deutsch, M. *Phys. Rev. E* **1997**, *55*, 3164.

(7) Zhang, Z.; Mitrinovic, D. M.; Williams, S. M.; Huang, Z.; Schlossman, M. L. *J. Chem. Phys.* **1999**, *110*, 7421.

(8) One modification from our earlier cleaning procedure is the use of hot (~70 °C) purified water for the final rinse of our sample cell before addition of the sample liquids.

(9) Goebel, A.; Lunkenheimer, K. *Langmuir* **1997**, *13*, 369.

(10) Schlossman, M. L.; Synal, D.; Guan, Y.; Meron, M.; Shea-McCarthy, G.; Huang, Z.; Acero, A.; Williams, S. M.; Rice, S. A.; Viccaro, P. J. *Rev. Sci. Instrum.* **1997**, *68*, 4372.

(11) Because the path length of the X-rays through the upper liquid phase varies as a function of the reflection angle, the absorption of the

X-rays varies with the angle α. This small correction is included in the analysis of the data and is approximately 3% at $Q_z = 0.25$ Å^{-1} (see ref 7).

(12) Nevot, L.; Croce, P. *Rev. Phys. Appl.* **1980**, *15*, 761.

(13) Sinha, S. K.; Sirota, E. B.; Garoff, S.; Stanley, H. B. *Phys. Rev. B* **1988**, *38*, 2297.

(14) Weeks, J. D. *J. Chem. Phys.* **1977**, *67*, 3106.

(15) Abraham, F. F. *Phys. Rep.* **1979**, *53*, 93.

(16) Braslau, A.; Deutsch, M.; Pershan, P. S.; Weiss, A. H.; Als-Nielsen, J.; Bohr, J. *Phys. Rev. Lett.* **1985**, *54*, 114.

(17) Braslau, A.; Pershan, P. S.; Swislow, G.; Ocko, B. M.; Als-Nielsen, J. *Phys. Rev. A* **1988**, *38*, 2457.

(18) Schwartz, D. K.; Schlossman, M. L.; Kawamoto, E. H.; Kellogg, G. J.; Pershan, P. S.; Ocko, B. M. *Phys. Rev. A* **1990**, *41*, 5687.

(19) Schlossman, M. L. *Structure of Surfaces and Interfaces of Fluids*; Trigg, G. L., Ed.; VCH Publishers: New York, 1997; Vol. 20, pp 311−336.

(20) Gelfand, M. P.; Fisher, M. E. *Physica A* **1990**, *166*, 1.

(21) Integration is over a circular region in reciprocal space, of radius $q_{max} = (2\pi/5)$ Å^{-1}, with a cutout in the center. The cutout is determined by the known resolution of the spectrometer, so that X-rays scattered by capillary waves with wave vectors $\boldsymbol{q}$ outside of the cutout region (thus, within the integration region) are deflected outside the angular acceptance of a detector centered on the position for specular reflection. For the values of σ_{cap} in Table 1, α is chosen to be 0.94° (corresponding to $Q_z = 0.25$ Å^{-1}) and $\Delta\beta = 0.6/676$ rads. We chose 5 Å, in the expression for q_{max} to correspond to the approximate chain−chain distance. However, the value of σ_{cap} is insensitive to the exact choice of q_{max}. For example, varying q_{max} by a factor of 2 results in a change of only 3% in σ_{cap}.

(22) Note that adjusting q_{max} to yield values of σ_{cap} in agreement with our measured values of σ would require using nonphysically large values of q_{max}.

(23) Eisenriegler, E. *J. Chem. Phys.* **1983**, *79*, 1052.

(24) Habenschuss, A.; Narten, A. H. *J. Chem. Phys.* **1989**, *91*, 4299.

(25) Habenschuss, A.; Narten, A. H. *J. Chem. Phys.* **1990**, *92*, 5692.

(26) Tkachenko, A. V.; Rabin, Y. *Phys. Rev. Lett.* **1996**, *76*, 2527.

(27) Earnshaw, J. C.; Hughes, C. J. *Phys. Rev. A* **1992**, *46*, R4494.

(28) Mitrinovic, D. M.; Tikhonov, A. M.; Li, M.; Huang, Z.; Schlossman, M. L. *Phys. Rev. Lett.* **2000**, in press.